Available online at www.sciencedirect.com
SCIENCE DIRECT®
Journal of Power Sources 124 (2003) 293–298
JOURNAL OF POWER SOURCES
www.elsevier.com/locate/jpowsour

Mathematic simulation on thermoelectric power generation with cylindrical multi-tubes

Ryosuke O. Suzuki [a,*], Daisuke Tanaka [a,b,1]

[a] Department of Energy Science and Technology, Kyoto University, Yoshida-honmachi, Sakyo-ku, Kyoto 606-8501, Japan
[b] Graduate School of Energy Science, Kyoto University, Yoshida-honmachi, Sakyo-ku, Kyoto 606-8501, Japan

Received 25 February 2003; received in revised form 27 May 2003; accepted 28 May 2003

Abstract

Analytical expression of electric power was deduced in case of the large-scale cylindrical thermoelectric tubes exposed to two thermal fluids. The output powers of the proposed six geometrical arrangements were mathematically solved from heat transfer theory, and compared with the flat panel systems. The maximum output was the largest in the ideally cooled systems. In the other realistic systems, it was the largest for the system of the counter flow with a single thermoelectric tube. The multiplication of thermoelectric panels can shorten significantly the device length, although the output from the multi-tubes decreases only a little. For example, the double helical tubes (T2CH system) can generate 96% output by 35% length, compared with the single tube in the counter flow (T1C system).

Keywords: Thermoelectric generation; Thermoelectric device; Heat transfer; Thermal fluid; Bismuth telluride

1. Introduction

In a large-scale power plant, a thermal energy is carried to the power generator. When it is extracted by a fluid and passed to the thermoelectric generator, a hot fluid offers the heat to the hot junctions in the thermoelectric modules. Seebeck effect can generate the thermoelectric power depending on a temperature difference between the hot and cold junctions. The thermoelectric motive force in the open circuit is the sum of multiplication of the relative Seebeck coefficient and the temperature difference ΔT over all the serial connections. The problem to obtain the larger power is, therefore, how to give the larger ΔT to all the thermoelectric panels existing between two hot and cold fluids [1–4].

The heat applied from a hot fluid is transferred to the panel surface, into the thermoelectric panel, and finally to the cold fluid at another surface. The two fluids are resultantly warmed or cooled along the flow paths, and their temperature profiles through the path, $T(x)$, change as a function of position, x. This problem is well known in heat exchanger through an isolator [5–7]. Additionally as the special feature in the thermoelectric power generation, the heat transfer due to Peltier effect and Joule heating should be considered [1,8,9].

The purpose of this work is to show the mathematical expression of the electric power extractable from the thermoelectric cylindrical tubes that are heated by a hot fluid and cooled by another cold fluid. Fig. 1 shows an example of this concept. The system of Fig. 1 consists of three thermoelectric tubes, in which two hot fluids and the two cold fluids flow as counter flow.

The previous studies showed that the maximum of output power exists corresponding to a certain module size [8–11]. It is because the longer serial connections of thermoelements can generate the higher voltage, but the extremely longer panels have the higher electrical resistivity and the temperature difference ΔT becomes smaller. For example, Kyono et al. evaluated the case when a single thermoelectric tube was isothermally cooled by the huge amount of coolant [10]. They reported that the maximum of 150 kW existed, although this optimum length was evaluated as a few hundreds km for FeAlSi–FeAl couple. However, this optimum size of the thermoelectric generator can be compacter in a few tens metre by using the high performance semiconductors such as Bi_2Te_3 [10,11].

It is expected that the multi-tubes, as illustrated in Fig. 1, can shorten the tube length and make the system more compact and suitable for the large-scale power generation, because the previous study showed that the necessary

* Corresponding author. Tel.: +81-75-753-5453; fax: +81-75-753-4745.
E-mail address: suzuki@energy.kyoto-u.ac.jp (R.O. Suzuki).
[1] Present address: Nomura Research Institute Ltd., Tokyo, Japan.

0378-7753/$ – see front matter © 2003 Elsevier B.V. All rights reserved.
doi:10.1016/S0378-7753(03)00626-8

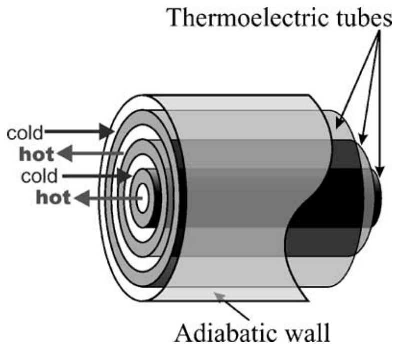

Fig. 1. Cylindrical multi-tube system.

panel area could be minimized when the thermoelectric flat multi-panels were connected three-dimensionally [11]. When the heat loss through a thermoelectric tube is recovered by another fluid, and when the captured heat is passed to another thermoelectric panel, we expect that the thermal energy can be efficiently recovered in a restricted space [2–4,8–11]. The cylindrical tubes consisting of the thermoelectric modules are suitable for circulation of the industrial fluids, such as exhaust hot gas or coolant water.

The analytical method for flat multi-panels [11] and that for a cylindrical tube [10] are here combined, and the heat transfer through the thermoelectric multi-tunes and the temperature change $T(x)$ along the fluid path with cylindrical symmetry are analyzed mathematically to discuss the maximum output power. Here we propose six types of thermoelectric power generation system with cylindrical multi-tubes.

2. Basic assumptions and models

2.1. Cylindrical thermoelectric tube

It is assumed that all of our thermoelectric modules are cylindrical, and that they consist of the thermoelements with a single layer of Π-type p–n junctions, as illustrated in Fig. 2(a). The thermoelements are homogeneously aligned perpendicular to heat flow, combined tightly without open space, and connected electrically in series. The hot and cold fluids are isolated by the panel, and flow along the both cylindrical surfaces of the panel. Practically, as shown in Fig. 2(a), there exist the electrodes connecting the thermoelements, the insulator between the elements, the protective insulating film on the electrodes, and the fins that enhance the heat exchange. Here for simplicity we neglected these effects on heat transfer, and considered them only as the heat transfer coefficient of the modules.

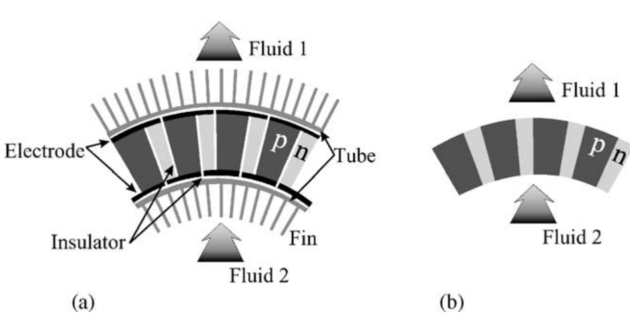

Fig. 2. Simplification of thermoelectric tube. (a) Practical model and (b) simplified model.

2.2. Directions of fluids

The number of the tubes, n, the directions of hot and cold fluids, and the path shape for fluids are classified systematically as shown in Fig. 3.

Firstly, three types of fluid direction are considered, depending on the direction of cold fluid at the outlet of the corresponding hot fluid: parallel flow type (P), counter flow type (C), and isothermal type (I). We assume only one path for each fluid. Namely, we set the boundary conditions that each system has only two paths connecting in series. No branched paths are considered, although it was one of the efficient methods as reported previously [11].

The parallel flow type is the system that the two fluids flow in the same direction, between which a thermoelectric panel is inserted. The fluids flow in the opposite direction at the counter flow type. These two types are often selected for heat exchangers using fluids [5–7]. The isothermal type is the extreme case that whole a surface of the most outside of the system is kept at a constant temperature by the infinitely large heat bath. This case for a single tube (T1I) was partially analyzed by Kyono et al. [10].

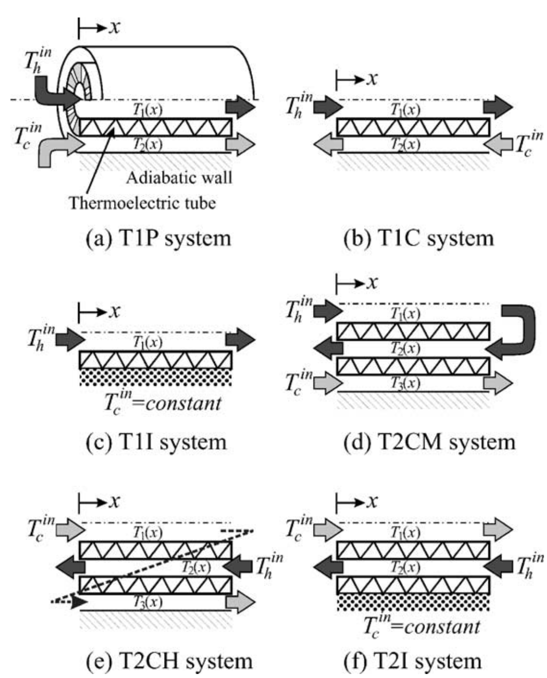

Fig. 3. Classification of thermoelectric systems.

Table 1
Conditions for the analyzed systems

System	Hydrodynamic conditions	Boundary conditions	In Fig. 3
T1P	$M_1 > 0,\ M_2 > 0$	$T_1(0) = T_h^{in},\ T_2(0) = T_c^{in}$	Fig. 3(a)
T1C	$M_1 > 0,\ M_2 < 0$	$T_1(0) = T_h^{in},\ T_2(l) = T_c^{in}$	Fig. 3(b)
T1I	$M_1 = M > 0$	$T_1(0) = T_h^{in},\ T_2(x) = T_c^{in}$ for all x	Fig. 3(c)
T2CM	$M_1 > 0,\ M_2 = -M_1,\ M_3 = M_1$	$T_1(0) = T_h^{in},\ T_1(l) = T_2(l),\ T_3(0) = T_c^{in}$	Fig. 3(d)
T2CH	$M_1 > 0,\ M_2 < 0,\ M_3 = M_1$	$T_1(0) = T_c^{in},\ T_2(l) = T_h^{in},\ T_3(0) = T_1(l)$	Fig. 3(e)
T2I	$M_1 > 0,\ M_2 < 0$	$T_1(0) = T_c^{in},\ T_2(l) = T_h^{in},\ T_3(x) = T_c^{in}$ for all x	Fig. 3(f)

2.3. Path shape

Secondly the path shapes of fluids are classified into meandering type (M) and helical type (H), as shown in Fig. 3. The meandering type and the helical type aim at the heat recycling and at the homogeneous ΔT for all the panels, respectively. The path connection is illustrated as broken lines in Fig. 3(e). The seamless three-dimensional connection is realized by bending the tube.

The analyzed tube (T) systems were named after the number of panel sheets (n), the direction of fluid flow (P, C or I) and the path shape (M or H). The hydrodynamic conditions and the boundary conditions are listed in Table 1.

3. Equations for output power

3.1. Deduction of equations

Our previous approach for multi-panels is applied for the multi-tubes [11]. The modification of heat transfer through the cylindrical thermoelectric tube is considered [10]. The circumferential homogeneous temperature is assumed that the turbulent flow is well developed inside the long path.

When the system consists of n tubes, a set of $n+1$ simultaneous derivative equations can be written from the heat transfers through tubes,

$$M_1 C_{p,1} \frac{dT_1(x)}{dx} = \mp K_1 (T_1(x) - T_2(x)) \tag{1}$$

$$M_i C_{p,i} \frac{dT_i(x)}{dx} = \pm K_{i-1}(T_{i-1}(x) - T_i(x)) \mp K_i (T_i(x) - T_{i+1}(x)) \quad (1 < i < n) \tag{2}$$

$$M_{n+1} C_{p,n+1} \frac{dT_{n+1}(x)}{dx} = \pm K_n (T_n(x) - T_{n+1}(x)) \tag{3}$$

where x is the position along the tube length. M_i, $C_{p,i}$ and T_i are mass flow rate, heat capacity and temperature for fluid i, respectively. The choice of $\pm$ depends on the path condition. K_i is the over-all heat transfer coefficient through the tube i in the direction perpendicular to x-axis,

$$K_i = \frac{2\pi}{(1/h_{i,i} r_{i,i}) + (\ln(r_{i+1}/r_i)/\lambda) + (1/h_{i+1,i} r_{i+1,i})} \tag{4}$$

r and h are the radius of the tube and the heat transfer coefficient between the fluid and the tube, respectively, as shown in Fig. 4. λ is the average heat conductivity of the tube, given by,

$$\lambda = \frac{\lambda_p \phi_p + \lambda_n \phi_n}{\phi_p + \phi_n} \tag{5}$$

where λ_p, λ_n, ϕ_p and ϕ_n are the heat conductivity and the angle of p- and n-type elements, respectively. For simplicity, heat transfer by Peltier effect and exothermal heat by Joule effect are neglected. This assumption leads to an overestimation for output power, although this overestimation is not significant, as we will report separately.

The equation is solved for x by setting the boundary conditions listed in Table 1. The temperature $\theta_{i,j}(x)$ at the surface of the panel i facing to the fluid j is then written using the solutions of simultaneous derivative equations, $T_i(x)$.

$$\theta_{i,i}(x) = T_i(x) - \frac{K_i}{h_i}(T_i(x) - T_{i+1}(x)) \tag{6}$$

$$\theta_{i,i+1}(x) = T_{i+1}(x) + \frac{K_i}{h_{i+1}}(T_i(x) - T_{i+1}(x)) \tag{7}$$

The electromotive force, E, is the summation of the temperature difference over all the panels,

$$E = \sum_{i=1}^{n} \left| n_\phi n_x \alpha \int_0^l (\theta_{i,i}(x) - \theta_{i,i+1}(x))\, dx \right| \tag{8}$$

where α is the difference between the Seebeck coefficients of p and n elements, n_ϕ and n_x are the number of thermoelectric pairs in a circumferential circulation, and the number density

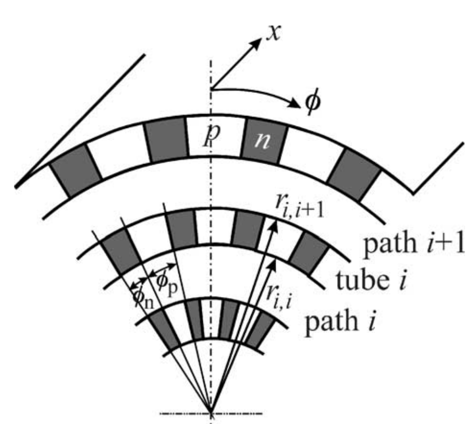

Fig. 4. Dimensions of thermoelectric tubes.

of the pairs in the direction x, respectively. Note that $n_\phi = 2\pi/(\phi_p + \phi_n)$. The electric resistance, R_i, is given as,

$$R_i = n_\phi {n_x}^2 l \left(\frac{\rho_p}{\phi_p} + \frac{\rho_n}{\phi_n}\right) \ln\left(\frac{r_{i,i+1}}{r_{i,i}}\right) \tag{9}$$

where ρ_p and ρ_n are the specific resistivity of p and n elements. The output power, P, is optimized by balancing the internal and external resistance,

$$P = \frac{E^2}{4\sum_{i=1}^{n} R_i} \tag{10}$$

This work uses hereafter this P, where the internal resistance is equal to the external resistance.

3.2. Output power of six systems

The simultaneous equations are solved at the T1P system, where one sheet of panel is exposed in parallel flow. The output was calculated by Eq. (10) as,

$$P_{T1P} = \frac{n_\phi n_x \{M_1 M_2 C_{p,1} C_{p,2} \alpha (T_h^{in} - T_c^{in})\}^2}{16(r_n + r_p) l} \times \left[\frac{K_{a1}\left\{e^{(-(1/M_1 C_{p,1}) - (1/M_2 C_{p,2}))Kl} - 1\right\}}{M_1 C_{p,1} + M_2 C_{p,2}}\right]^2 \tag{11}$$

where r_n and r_p are the resistivity for n- and p-type, respectively, in one unit of thermocouple. The output P_{T1P} had been maximized using the conditions that,

$$\phi_n = \frac{2\pi\sqrt{\lambda_p \rho_n}}{n_\phi(\sqrt{\lambda_n \rho_p} + \sqrt{\lambda_p \rho_n})} \quad \text{and}$$

$$\phi_p = \frac{2\pi\sqrt{\lambda_n \rho_p}}{n_\phi(\sqrt{\lambda_n \rho_p} + \sqrt{\lambda_p \rho_n})} \tag{12}$$

and the new parameter K_{a1} was defined relating with heat flow through the panel as,

$$K_{a1} = \frac{h_{11} K_1 r_{11} + h_{12} K_1 r_{12} - 2\pi h_{11} h_{12} r_{11} r_{12}}{\pi h_{11} h_{12} K_1 r_{11} r_{12}} = \frac{\ln(r_{12}/r_{11})}{\pi \lambda_1} \tag{13}$$

The same optimized conditions for ϕ_n and ϕ_p were also used in the following calculations.

The solutions for T1C system were generally given as,

$$P_{T1C} = \frac{n_\phi n_x \{M_1 M_2 C_{p,1} C_{p,2} \alpha (T_h^{in} - T_c^{in})\}^2}{16(r_n + r_p) l} \times \left[\frac{K_{a1}\left\{e^{(-(1/M_1 C_{p,1}) - (1/M_2 C_{p,2}))Kl} - 1\right\}}{M_1 C_{p,1} e^{(-(1/M_1 C_{p,1}) - (1/M_2 C_{p,2}))Kl} + M_2 C_{p,2}}\right]^2 \tag{14}$$

When $M_1 C_{p,1} = -M_2 C_{p,2} = MC_p$, however, the special care was needed in solving the differential equations. The output power of this case,

$$P_{T1C} = \frac{n_\phi n_x \{MC_p \alpha (T_h^{in} - T_c^{in})\}^2 l}{16(r_n + r_p)} \left[\frac{K_{a1}}{MC_p + Kl}\right]^2, \tag{15}$$

was equal to the infinite expression of Eq. (13) when $M_1 C_{p,1}$ approaches to $-M_2 C_{p,2}$.

The solutions for T1I system was given as,

$$P_{T1I} = \frac{n_\phi n_x \{MC_p \alpha (T_h^{in} - T_c^{in})\}^2}{16(r_n + r_p) l} [K_{a1}(1 - e^{-(Kl/MC_p)})]^2 \tag{16}$$

Eq. (16) is the infinite expression when $M_2 C_{p,2}$ is infinitely large in either Eq. (11) or (14). It is natural because the T1I system holds the infinitely large heat bath, which is made possible by supply of an infinitely large amount of fluid. Eq. (16) essentially agreed with the previous report [10], although the definitions of the symbols were different.

In the solutions for the double-tubes systems, we will report only the case of $|M_1 C_{p,1}| = |M_2 C_{p,2}| = |M_3 C_{p,3}| = MC_p$ for simplicity,

$$P_{T2CM} = \frac{n_\phi n_x \{MC_p \alpha (T_h^{in} - T_c^{in})\}^2}{2(r_{n1} + r_{n2} + r_{p1} + r_{p2}) l} \times \frac{[\sin h(X)\{K_{a1}\sqrt{K_1}\sinh(X) + K_{a2}\sqrt{K_2}\cosh(X)\}]^2}{\sqrt{K_1}\cosh(2X) + \sqrt{K_2}\sinh(2X)} \tag{17}$$

where K_{a2} and X were defined as,

$$K_{a2} = \frac{h_{22} K_2 r_{22} + h_{23} K_2 r_{23} - 2\pi h_{22} h_{23} r_{22} r_{23}}{\pi h_{22} h_{23} K_2 r_{22} r_{23}} = \frac{\ln(r_{23}/r_{22})}{\pi \lambda_2} \tag{18}$$

and

$$X = \frac{l\sqrt{K_1 K_2}}{2MC_p} \tag{19}$$

respectively. Using the same parameters,

$$P_{T2CH} = \frac{n_\phi n_x \{MC_p \alpha (T_h^{in} - T_c^{in}) \sinh(X)\}^2}{4(r_{n1} + r_{n2} + r_{p1} + r_{p2})(K_{a1} - K_{a2}) l} \times \left[\frac{\{(K_1 K_{a1} + K_2 K_{a2})\cosh(X) + \sqrt{K_1 K_2}(K_{a1} - K_{a2})\sinh(X)\}}{\sqrt{K_1 K_2}\cosh(2X) + (K_1 + K_2)\sinh(2X)}\right]^2 \tag{20}$$

and

$$P_{T2I} = \frac{n_\phi n_x \{MC_p \alpha (T_h^{in} - T_c^{in})\}^2}{16(r_{n1} + r_{n2} + r_{p1} + r_{p2}) l} \times \left[\frac{\sqrt{K_2(4K_1 + K_2)} K_{a2}\{\cosh(Z) - e^{-Y}\} + (2K_1 K_{a1} + K_2 K_{a2})\sinh(Z)}{\sqrt{K_2(4K_1 + K_2)}\cosh(Z) + (2K_1 + K_2)\sinh(Z)}\right]^2 \tag{21}$$

where

$$Y = \sqrt{\frac{K_2}{K_1}} X \quad \text{and} \quad Z = \sqrt{4 + \frac{K_2}{K_1}} X \tag{22}$$

The obtained expressions contain the common term of $n_\phi n_x\{M_1 M_2 C_{p,1} C_{p,2} \alpha (T_h^{in} - T_c^{in})\}^2$. The other parts depend on the geometry of the system, electric resistivity and heat transfer coefficient K_i. K_i depends on the radius of thermoelectric panel in the cylindrical system. This is unable to simplify the expressions, while the output power of the flat multi-panels systems could be expressed by the non-dimensional parameters [11]. Therefore, the obtained output for six systems will be numerically compared using the thermophysical values of Bi_2Te_3 semiconductors.

4. Physical properties and conditions

The thermophysical properties of the BiTe thermoelectric elements in the literature scattered due to the impurities, their temperature dependencies and the difference in preparation [1,12]. Table 2 shows a typical set of properties for an identical sample at room temperature [1], and used for this work. Table 3 shows the fluid properties [6,7,13] and the parameters for thermoelectric tubes. The thickness of thermoelectric elements was set as 0.05 m based on the previous discussion [11]. The most inner radius was set as 0.1 m, and the path width (the gap between cylindrical two tubes) 0.1 m. The other thermophysical properties and conditional parameters are identical with the previous work [11], and the temperature dependencies of these values are not considered.

Table 2
Specific values of thermoelectric elements used here

Materials	Seebeck coefficient, α (μV/K)	Resistivity, ρ (μΩ m)	Thermal conductivity, λ (W/Km)	Figure of merit, Z (1/K)
Bi–54.3 at.% Te (p)	162	5.55	2.06	2.605×10^{-3}
Bi–64.5 at.% Te (n)	−240	10.1	2.02	

Table 3
Parameters for thermoelectric power generation system

	Variables	Values used in this work
Thermoelectric device	Length, l	Variable
	Thickness of tube, d	0.05 m
	Radius of inner tube, r_1	0.1 m
	Distance between two tubes (thickness of fluid path)	0.1 m
	Number density of pairs, n_x	50/m
	Number of pairs, n_ϕ	100/cylinder
Thermal sources	Hot source	N_2 gas (inlet $T_h^{in} = 500$ K)
	Cold source	N_2 gas (inlet $T_c^{in} = 300$ K)
Gas properties	Specific heat, $C_{p,hot} = C_{p,cool}$	1044 J/(kg K) (at 400 K, 0.1 Pa)
	Mass flow rate, $M_{hot} = M_{cool}$	1.00 kg/s
	Heat transfer coefficient, $h_{hot} = h_{cool}$	500 W/(m^2 K)

5. Comparison of multi-tube systems

Fig. 5 shows the output power thus evaluated for six systems. The output power of each system became the maximum at a certain length. This maximum output power, P^{max}, and its system length, L^{max}, are listed in Table 4. P^{max} was the largest for T1I system, i.e. $P_{T1I}^{max} = 9.49$ kW at $L^{max} = 48.5$ m. However, the isothermal heat sink in the T1I system is an ideal case, and it is practically impossible to supply the fluid at the infinitely fast rate in order to keep isothermal. When we feed the hot and cool fluids at the same finite rate (i.e. $|M_{hot}| = |M_{cool}|$), P_{T1P}^{max} and P_{T1C}^{max} were evaluated to be 50 and 61.3%, respectively, of P_{T1I}^{max}. This means that the unbalanced flow rate can generate larger power than P_{T1P}^{max} and P_{T1C}^{max} shown in Fig. 5, and the power approaches to P_{T1I}^{max} when the flow rate of a fluid increases keeping the another constant. The fact that P_{T1C}^{max} was larger than P_{T1P}^{max} is consistent with the flat multi-panels [11]. Therefore, only counter flow type was considered for the double tube systems.

P_{T2CH}^{max} was 96.0% of P_{T1C}^{max}, while L_{T2CH}^{max} was only 35.2% of L_{T1C}^{max}. From the viewpoint of the more compact system to reduce the required modules and the space, the multiple tube systems are more effective, and the T2CH system seems the most economic for construction. These tendencies are similar with the system with the multiple flat-panels [11]. The multi-tubes systems such as T3CH or T4CH systems seem worth for further consideration.

For comparison with the flat panel systems in the previous study [11], P^{max} was evaluated in Table 4 using the identical data in Tables 2 and 3. P^{max} of the systems with one cylindrical tube (T1 types) are as large as those of one flat panel systems (F1 types). However, the cylindrical systems with double-tubes (T2CM and T2I) cannot generate the larger output than the double flat panels systems (F2CM and F2I), except for the helical type. The reason is as the follows. The over-all heat transfer through the tube is roughly proportional to the tube radius. Therefore, the heat transfer

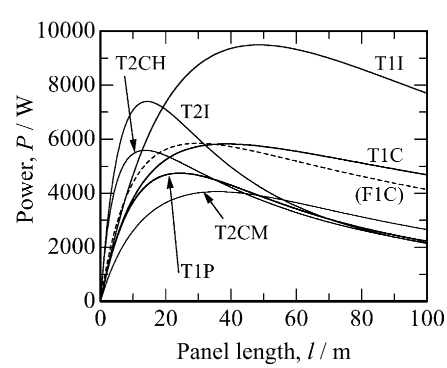

Fig. 5. Output power of multi-tube system.

Table 4
Output power and system length when the output power becomes maximum

System [11]	Maximum output power, P^{max} (kW)	System length, L^{max} (m)	System	Maximum output power, P^{max} (kW)	System length L^{max} (m)
F1P	4.763	18.72	T1P	4.744	24.26
F1C	5.847	29.80	T1C	5.825	38.61
F1I	9.525	37.44	T1I	9.489	48.51
F2CM	4.763	37.44	T2CM	4.057	35.74
F2CH	5.453	12.39	T2CH	5.589	13.64
F2I	8.594	19.40	T2I	7.397	14.29

of the outer tube becomes larger, and the larger amount of heat passes through the outer panel. Therefore the fluid temperature changes more quickly along the outer path, and the temperature difference between the fluids becomes smaller at the outer panel. This phenomenon reduces the electromotive force, E, especially in the systems such as T2CM and T2I.

P^{max}_{T2CH} was 2.50% larger than P^{max}_{F2CH}, as listed in Table 4. This is because the helical type gives a homogeneous temperature difference over the whole panel length. This homogeneous temperature distribution does not enhance the heat flow through the outer panel. Then the temperature difference on the thermoelectric modules become larger and the output power increases. The helical type has the potential of the larger output by increasing the number of panels.

The meandering type did not show any good output and miniaturization. This is because of the assumption that all the thermoelectric modules were connected in series and that all panels were the same length. If we can control the panel length of two panels independently, we may optimize the output power of the individual panel.

6. Conclusion

This work studied the thermoelectric power generation with cylindrical multi-tubes in which thermoelectric elements were embedded. Six systems were analyzed using the heat transfer theory and their output powers were expressed in the analytical mathematic equations. Because the over-all heat transfer coefficient depends on the tube radius, these equations are more complex than those of the flat multi-panels.

The maximum output power, P^{max}, was obtained at the T1I system where the cold surface was kept isothermally by the infinitively large heat sink. P^{max}_{T1C} is the largest in the other five realistic systems, although the length necessary for the maximum output is longer than those for double tubes systems. The helical type with two tubes (T2CH) can generate as large as the T1C system, and L^{max}_{T2CH} is significantly shorter than that for T1C system. The helical type with the multi-tubes makes the system compacter, keeping high P^{max}.

Acknowledgements

The authors thank to Mr. Takashi Kyono for useful discussions. This work was supported in part by Japan Nuclear Cycle Development Institute (JNC), Yazaki Memorial Foundation for Science and Technology, and Sekisui Chemical Co. Ltd.

References

[1] R. Sakata (Ed.), Thermoelectrics, Principles and Applications, Realize Inc., Tokyo, 2001.
[2] K. Ono, R.O. Suzuki, R. Nakahashi, M. Shoda, Tetsu-to-Hagané 83 (2) (1997) 157–161.
[3] K. Ono, R.O. Suzuki, in: Proceedings of the 17th International Conference on Thermoelectrics, IEEE, Piscataway, NJ, 1998, pp. 515–518.
[4] K. Ono, R.O. Suzuki, J. Metals (December) (1998) 49–51.
[5] S. Isshiki, N. Kitayama, Technology of Heat Transfer, Morikita Press, Tokyo, 1984.
[6] W.M. Kays, M.E. Crawford, Convective Heat and Mass Transfer, second ed., McGraw-Hill, New York, 1980.
[7] Heat Transfer, fourth ed., Japanese Society of Mechanical Engineers, Tokyo, 1986.
[8] B. Mathiprakasam, T. Sutikno, J. Beeson, in: Proceedings of the Fourth International Conference on Thermoelectrics, IEEE, Piscataway, NJ, 1982, p. 61.
[9] J. Esarte, G. Min, D.M. Rowe, J. Power Sources 93 (2001) 72–76.
[10] T. Kyono, R.O. Suzuki, K. Ono, IEEE Trans. Energy Conv. 18 (2) (2003) 330–334.
[11] R.O. Suzuki, D. Tanaka, J. Power Sources 122 (2) (2003) 201–209.
[12] D.M. Rowe, CRC Handbook of Thermoelectrics, CRC Press, Boca Raton, 1995.
[13] Thermophysical Properties of Fluids, Japanese Society of Mechanical Engineers, Tokyo, 1986.